Mechanical and Tribological Performance of *Luffa cylindrica* Fibre-Reinforced Epoxy Composite

Niharika Mohanta* and Samir K. Acharya

This work focuses on the mechanical properties and solid particle impact behaviour of *Luffa cylindrica* fibre (LCF)-reinforced epoxy composites. Single (SL)-, double (DL)-, and triple (TL)-layered composites were prepared using the general hand lay-up technique. The erosive wear test was carried out using an air jet erosion tester according to the ASTM G76 standard. The erodent used was silica sand particles (200 ± 50 µm). The experimental parameters studied for the erosion rate of the LCF epoxy composites were impingement angle (30° to 90°) and particle velocity (48 m/s to 82 m/s). Analysis of the results revealed that at the peak erosion rate, semi ductile behaviour of the composite was apparent. Possible erosion mechanisms were discussed and were investigated using scanning electron microscopy (SEM).

Keywords: Luffa cylindrica fibre (LCF); Mechanical properties; Erosive wear; Erodent; Semi-ductile; SEM

Contact information: Department of Mechanical Engineering, NIT Rourkela-769008, Odisha, India;
** Corresponding author: mohanta.niharika@gmail.com*

INTRODUCTION

Fibre-reinforced composites are widely used as components in engineering structures because of their enhanced stiffness and strength properties in comparison to traditional materials (Rout *et al.* 2001; Li and Matuana 2003). However, increasing concern for greenhouse gas effects and environmental awareness is limiting their use in the industry. Alternatively, over the last few years, natural fibres have been chosen by researchers as a reinforcement material to replace synthetic fibres in polymer composites. Reinforced materials are economical in price and a favourable option from an ecological prospective. Fibre-reinforced composites have been widely used in aerospace applications. Most of the industrial and manufacturing components are exposed to tribological loading, such as adhesives, abrasives, *etc*., during various types of service. Therefore, it is important to study the tribological performance of a material while designing a mechanical component. Similarly, for natural fibre-reinforced composites, it is essential to study the mechanical and tribological behaviour before they are considered for a particular use.

Many studies have emphasised the erosion behaviour of natural composites, generating the opinion that erosion is not only an intrinsic behaviour of natural fibre, but is also strongly dependent on many operating parameters (Deo and Acharya 2009; Mishra and Acharya 2010; Gupta *et al.* 2011; Patel *et al.* 2011; Mohanty *et al.* 2014).

Luffa cylindrica (L.) synonym L. aegyptiaca Mill, a forest product commonly called sponge gourd, loofa, vegetable sponge or bath sponge, is a member of the cucurbitaceous family (Mazali and Alves 2005). It is a subtropical plant abundantly available in Japan, China, India, and other countries in Asia as well as in Central and South America (Oboh and Aluyor 2009). The fruit of *Luffa cylindrica* can be eaten as a vegetable when it is young. But mature fruits cannot be eaten because of their bitter taste due to development of purgative chemicals. Due to its purgative property, *Luffa cylindrica* is used as medicine for remedy of dropsy, nephritis, and chronic bronchitis and lung complaints (Partap *et al.* 2012). The *Luffa* fruit has a fibrous, vascular system that forms a natural mat when dried, and it has a unique knitting structure which is generally not found in other natural fiber as shown in Fig. 1. The natural luffa mat possesses remarkable strength, stiffness, and energy absorption capacity comparable to metallic cellular material in a similar density range (Shen *et al.* 2012). Like other natural fibres, *Luffa cylindrica* fibre (LCF) contains cellulose (62.0%), hemicellulose (20%), lignin (11.2%), ash (0.40%), and extracts (3.1%) (Satyanarayana *et al.* 2007). Previous studies of this fibre primarily relate to the flexural properties of both treated and untreated fibres reinforced polymer composite (Boynard *et al.* 2003; Ghali *et al.* 2011).

There is no information available in the literature concerning the erosive wear behavior of LCF-reinforced polymer composites. Hence, the priority of this study focuses on how to prepare a polymer matrix composite (PMC) using LCF as the reinforcement material and to determine the erosive wear behaviour by studying several parameters. Several researchers have correlated the erosion rate of composites with some important factors, such as the target materials, operating parameters, properties of the erodent, and the testing environment (Tewari *et al.* 2002; Bhushan *et al.* 2013). In the present study, experiments were carried out to evaluate the effect of impingement angle and particle velocity on the erosive wear behaviour of LCF-reinforced composites. Also, the mechanical properties of the LCF-reinforced composites were reported in this study.

EXPERIMENTAL

Raw Materials

Luffa cylindrica fibres were extracted from the sponge guard that were collected locally in Rourkela, Odisha, India. The LCFs were cut to rectangular sizes to be used in the preparation of the composite. Fig.1 shows the luffa fibre mat from which the LCF samples were cut. The details of the fibre preparation are given in (Mohanta and Acharya *et al.* 2013). The epoxy resin LY556 (diglycidyl ether of bisphenol A) was used as the matrix material. The epoxy resin and the hardener HY 951 were mixed at a ratio of 10:1 (wt. %). Both the epoxy resin and hardener were supplied by Hindustan Ciba Geigy Ltd., Mumbai.

Fig. 1. The rectangular portion of the natural *Luffa cylindrica* mat used in the preparation of the composites

Composite Fabrication

The conventional hand lay-up technique was used to fabricate composites having single (SL), double (DL), and triple (TL) layers of LCF fibre in three different weight proportions (8 wt. %, 13 wt. %, and 19 wt. %). For different wt. % of fibres, a calculated amount of epoxy resin and hardener (ratio of 10:1 by weight) was thoroughly mixed with gentle stirring to minimize air entrapment. Different layers of luffa fibres were kept in a mould with the dimensions 140 mm x 100 mm x 6 mm under uniform load after pouring the epoxy and hardener mix into the mould. The composites were cured for 48 h at room temperature and post-cured for another 24 h after the removal from the mould. For easy removal of the composites, sheets of Teflon® and silicon spray were used, which prevented any adhesion between the mould wall and the composite. Specimens of the required dimensions were cut using a diamond cutter for use in the mechanical and erosion testing experiments.

Methods

Mechanical properties of LCF-reinforced composites

A Contech precision analytical balance (Contech Instruments Ltd., Maharashtra, India) was used to measure the density of the composites using the Archimedes principle (Ojha *et al.* 2014). A universal testing machine (UTM; H10KS, Hounsfield Test Equipment Ltd, England,) was used to determine the tensile strength and elongation of break according to the ASTM D 3039M-14 (2014) standard procedure. Initial grip separation was set to 42 mm, and a crosshead speed of 2 mm/min with a 10 KN load cell was employed. Five samples were tested, and the average was reported for each of the composite sample groups: neat epoxy, SL, DL, and TL.

The same UTM was utilised to determine the flexural strength and the interlaminar shear strength, according to ASTM D790-03 (2003). The span to depth ratio was set to 16:1, and a crosshead speed of 2 mm/min with 10 KN load cell was employed. Five samples were tested for each type of composite, and the mean values were reported The impact strength of the composites was measured using an IZOD impact tester (Veekay Test lab, Mumbai, Maharashtra, India), according to ASTM D256-10 (2010). Five samples for each type of composite were tested, and the mean values of impact strength were reported.

A Micro-Vickers hardness testing system (LV 700, LECO Co. Michigan, and USA) was used to measure the micro hardness of all the composite samples, according to the ASTM D 384-11e1 (2011) standard, performed at room temperature. Five indentations on each sample were used to calculate the mean hardness value for each of the composite samples.

Erosion wear test

In the solid particle erosion experiment, two methods were used to predict the erosion rate: the sand blast method, and the whirling arm method. A sand blast-type machine (Magnum Engineers, Bangalore, India) was used for this test. The test apparatus was designed to be representative of an erosive situation over a wide range of particle sizes, particle fluxes, impact velocities, and impact angles. The schematic of the air jet erosion test apparatus used for the study is shown in Fig. 2. The air jet erosion test apparatus consisted of a 4-mm-diameter nozzle with a length of 30 mm. The erodent was fed from a hopper by gravity through a conveyor belt system into the air particle mixing chamber and was accelerated by passing through the converging nozzle to bombard the specimen.

The impact velocity was measured according to the standard double disc method (Ruff and Ives 1975). The details of impact velocity calibration at various pressures obtained by this method are given in Table 1.

The room-temperature solid particle erosion test on SL, DL, and TL LCF-reinforced epoxy composites was carried out at impingement angles ranging from 30 to 90°. Dry silica particles (supplied by Magnum Engineers, Bangalore, India) of 250 ± 50 µm were used as the erodent. The erosion test was conducted according to the ASTM G76-13 (2013) standard. The amount of wear was estimated by measuring the weight loss after each run. The samples were cleaned using a soft brush to avoid entrapment of wear debris if any during experimentation. The steady state erosion rate (g/g) (E_r) was calculated using Eq. 1,

$$E_r = \frac{\Delta W_c}{\Delta W_s} \quad (1)$$

where ΔW_c is the weight loss of the composite (g) and ΔW_s is the total weight of erodent used (g). The test conditions under which the experiment was carried out are given in Table 2.

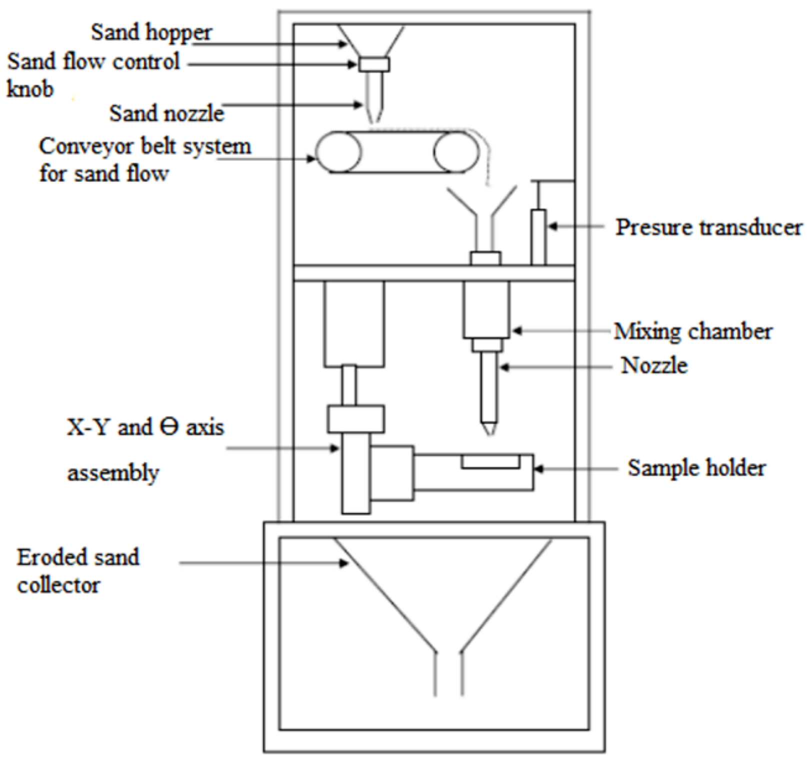

Fig. 2. Schematic diagram of the air jet erosion test apparatus

Scanning electron microscopy

Scanning electron microscopy (SEM; JEOL JSM-6480 LV, Japan Electronic Operated Limited, Japan) was used to examine the morphology of the eroded surfaces of composites. The composite samples were fixed on stubs with silver paste and coated with a thin film of platinum to enhance the conductivity before the photomicrographs were taken.

Table 1. Impact velocity calibration at various pressures

Pressure (bar)	Speed of rotating disc(rpm)	Angle θ (°)	Velocity(m/s)	Avg. impact velocity(m/s)
1	2000	7	42.85	47.25
		6.5	46.15	
		6	50.00	
		6	50.00	
2	2000	4	75.00	69.16
		4.5	66.67	
		4	75.00	
		5	60.00	
3	2000	4.5	66.67	81.845
		4	75.00	
		3.5	85.71	
		3	100.00	

Table 2. Testing Conditions for the Erosion

Erodent	Silica sand
Erodent size (µm)	200 ± 50
Erodent shape	irregular
Impingement angle (°)	30, 45, 60, 90
Impact velocity(m/s)	48, 70, 82
Erodent feed rate (gm/min)	10
Test temp (°C)	27
Nozzle to sample distance (mm)	20

RESULTS AND DISCUSSION

Mechanical Properties

The densities of composites obtained for the present study, along with other mechanical properties, are shown in Table 3. The actual density of the *Luffa cylindrica* epoxy composite decreased with increasing the layers of *Luffa cylindrica* fibre as compared to neat epoxy, as shown in Table 3. This is due to the low density of *Luffa cylindrica* fibre, *i.e.* 0.56 g/cm^3. The tensile strength, flexural strength, and impact strength of the SL, DL, and TL composites are presented in Table 3. From the table it is clearly observable that the strength properties of composite were increasing with increase in fiber loading up to double layer (DL) of luffa fiber. However there was a decrease in strength property for TL composite. This may be due to poor fiber wetting with matrix material, leading to poor fiber-matrix adhesion that might have promoted micro-crack formation at the interface as well as non-uniform stress transfer due to fiber agglomeration within the matrix (Karmarkar *et al.* 2007; El-Shekeil *et al*. 2012).

The interlaminar shear strength was found to be appreciably increased for SL, DL, and TL LCF-epoxy composites in comparisons to neat epoxy, as presented in Table 3. From the table it is also observed that there was a gradual increase in micro hardness for

SL and DL composites. However there was a decrease in hardness for TL composite. The variation in the observed behaviour may be due to the presence of voids.

Table 3. Mechanical and Physical Properties of LCF-Reinforced Composites

Composite type	Neat epoxy	Single layer (SL)	Double layer (DL)	Triple layer (TL)
Density (g/cm^3)	1.20	1.03	0.98	0.97
Tensile strength (MPa)	13.50	16.50	18.00	15.00
Elongation (%)	1.11	4.19	4.78	4.50
Tensile modulus (MPa)	521	650	699	725
Flexural strength (MPa)	17	24	28	26
Impact strength (kJ/m^2)	2.50	3.90	4.90	4.00
ILSS (MPa)	0.60	0.64	1.01	1.38
Hardness (MPa)	153.15	198.10	217.20	210.10

Erosion Rate

Influence of impingement angle (α) on the erosion wear behavior

Figure 3(a-c) shows the influence of the impingement angle (α) on the erosion rate of the SL, DL, and TL LCF-reinforced epoxy composites at various impact velocities. The results demonstrated that the erosion rate increased with increasing impingement angle (α), obtaining a maximum value at a 45° impingement angle for the SL and DL composites. However, the erosion rate achieved a maximum at an impingement angle of 60° for the TL composite. Materials are categorized as ductile or brittle based on the dependence of their erosion rate on the impingement angle (Arjula and Harsha 2006). If the peak erosion rate takes place at a low impingement angle (typically between 15 and 30°), then the material is classified as ductile. On the other hand, if the maximum erosion occurs at a 90° impingement angle, then the material is classified as brittle.

As evident from literature and pointed out by Rattan and Bijwe (2007), there were no fixed trends correlating the ductility and brittleness of a material with maximum or minimum erosion rate at various impingement angles. However, thermoplastics generally exhibit a more ductile response than do thermosets. Deo and Acharya (2009), while studying the erosion behavior of *Lantana camara* fibres-reinforced epoxy composite, found that the maximum erosion rate occurred at 45°, showing semi-ductile behaviour. For the present study, the maximum erosion occurred for the various layered composites in the range of 45 to 60°. Hence, it was concluded that the present LCF-reinforced epoxy composites behaved in a semi-ductile manner. The same type of behaviour was also reported in the literature for other natural fibre composites (Mohanty *et al.* 2014; Shakuntala *et al.* 2014).

However the interesting point here is that for higher fiber loading (TL) LCF-epoxy composite the maximum erosion rate was shifted from 45^o towards 60^o impact angle for all impact velocities. This gives an indication that the ductile behavior of the composite shifted towards the brittle behavior (Samantarai and Acharya 2015).

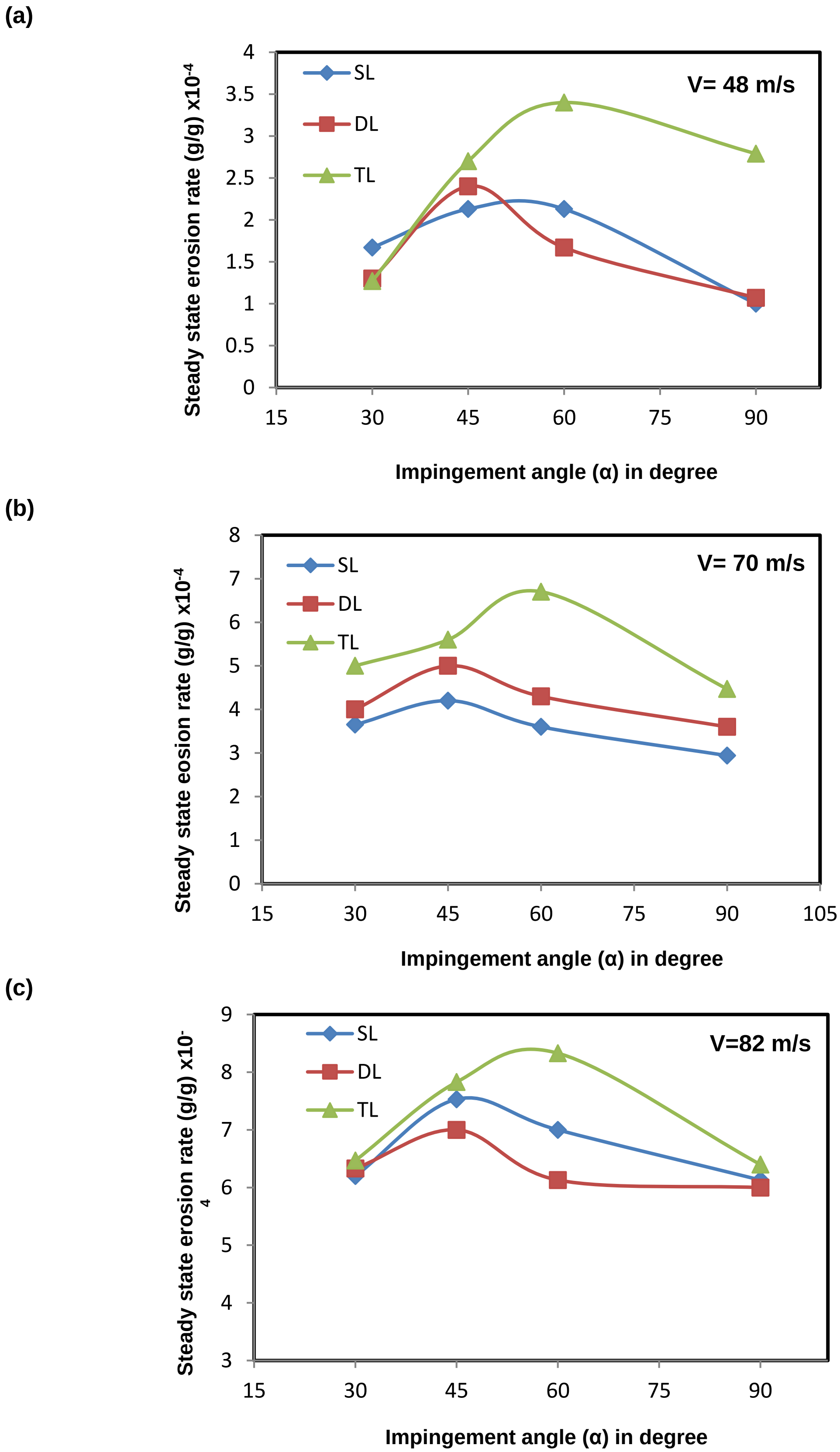

Fig. 3. The erosion rate as a function of the impingement angle (α) for LCF-reinforced epoxy composites at impact velocities of (a) 48 m/s, (b) 70 m/s, and (c) 82 m/s

Influence of impact velocity on erosion wear behavior

Figure 4(a,b) shows the results of the erosion rate for the same LCF-reinforced epoxy composites as a function of the impact velocity. It is clear from the figure that the steady-state erosion rates of the LCF-reinforced epoxy composites increased with increasing impact velocity at the various impingement angles. Results of the solid particle impact experiment showed that the impact velocity of the erosive particles exhibited a very strong effect on the erosion rate.

(a)

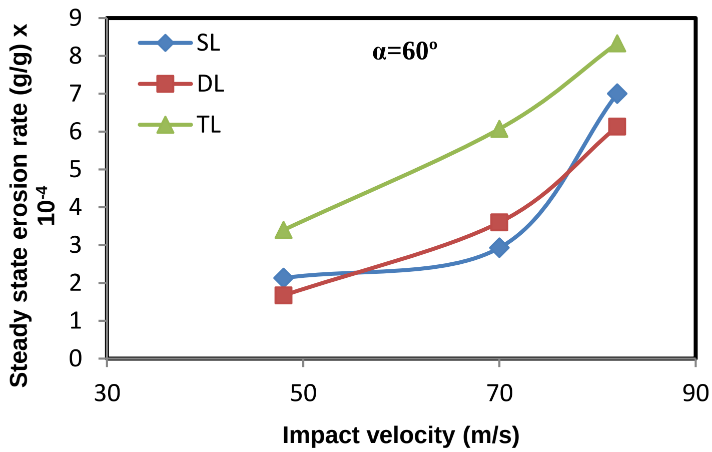

(b)

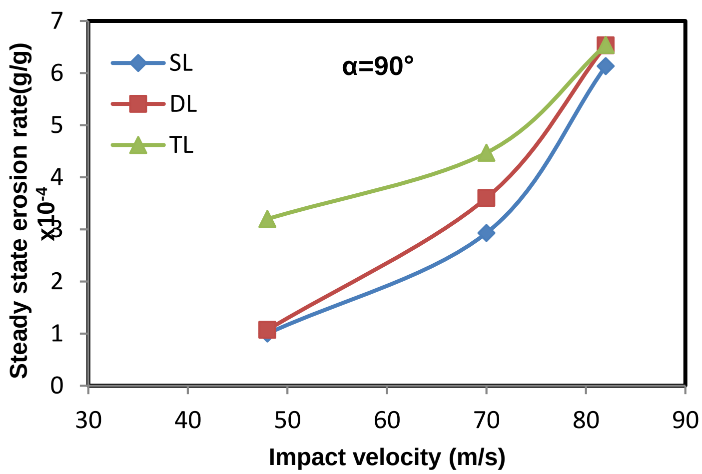

Fig. 4. The variation in steady state erosion rate of the LCF epoxy composites as a function of the impact velocity (48 to 82 m/s) at impingement angles of (a) 60° and (b) 90°

For any material, once steady-state conditions have been reached, the erosion rate (E_r) can be expressed as a simple power function of impact velocity (v) (Pool *et al.* 1986), as shown in Eq. 2,

$$E_r = kv^n \tag{2}$$

where k is proportionality constant and n is the velocity exponent. The least-squares fits to the data points were obtained were obtained using the power law (Eq. 2), and the values for n and k are summarized in Table 4. The velocity exponent n was found in the range of 1.3 to 3.3 for the various layered composites at various impingement angles. Pool *et al.*

(1986) reported that for polymeric materials behaving in a ductile manner, *n* typically lies between 2.0 and 3.0, while for polymer composites behaving in a brittle manner, *n* values between 3.0 and 5.0 could be expected. For the present study, as *n* varied from 1.3 to 3.3, it can be concluded that the LCF-reinforced composites exhibited semi-ductile behaviour. Similar results are also observed by Mohanty *et al*. (2014) in their study of date palm reinforced epoxy composite.

Table 4. Parameters Characterizing the Velocity Dependence of the Erosion Rate of LCF-Reinforced Composites

Composite type	Impingement angle (º)	*K*	*n*	R^2
Single layer	30	1.0 E-08	2.44	0.99
	45	3.0 E-08	2.26	0.96
	60	9.0 E-08	1.97	0.78
	90	3.0 E-10	3.29	0.98
Double layer	30	1.0 E-09	2.97	0.99
	45	1.0 E-07	1.99	0.99
	60	2.0 E-08	2.36	0.98
	90	2.0 E-10	3.35	0.99
Triple layer	30	2.0 E-05	1.25	0.93
	45	1.0 E-08	2.54	0.99
	60	6.0 E-07	1.65	0.99
	90	2.0 E-06	1.25	0.93

Erosion Efficiency

The ductile and brittle responses of the various materials relative to solid particle erosion were identified using the erosion efficiency (η) parameter, which was proposed by Sundararajan *et al*. (1990). The erosion efficiency (η) was obtained using Eq. 3.

$$\eta = \frac{2E_r H}{\rho v^2} \tag{3}$$

where E_r is the steady-state erosion rate (m/s), H is the hardness (MPa), ρ is the density of the target material (g/cm^3), and v is the velocity of an impinging particle (m/s). The erosion efficiencies of the LCF-reinforced epoxy composites were calculated using Eq. 3 for the various impact velocities. The results are shown graphically in Fig. 5(a, b). It was found that the erosion efficiency (η) of the SL and DL composites increased with increasing velocity of the impinging particles. However, the opposite was true for the TL composites: the erosion efficiency decreased with increasing impact velocity. Similar types of results are also reported by Srivastava and Pawar (2006). The lower value of erosion efficiency for the SL composites at various impact velocities indicated a favourable erosion resistance. Higher values for the TL composites indicated a poor erosion resistance (Harsha and Thakre 2007). The erosion efficiencies of LCF-reinforced epoxy composites varied from 1.67% to 4.83% for the impact velocities studied at a 90° impact angle (Fig. 5a) and

2.30% to 5.13% at a 60° impact angle (Fig. 5b). Thus, by observing the erosion efficiency and the velocity exponent (*n*), the erosion response of the LCF-reinforced epoxy composites can be broadly categorized as semi-ductile. This conclusion was drawn by following the classifications made by Sundararajan *et al.* (1990). Similar observations of the erosion efficiency for different polymeric composites have also been reported in the literature (Satapathy *et al.* 2009; Mohanty *et al.* 2014).

(a)

(b)

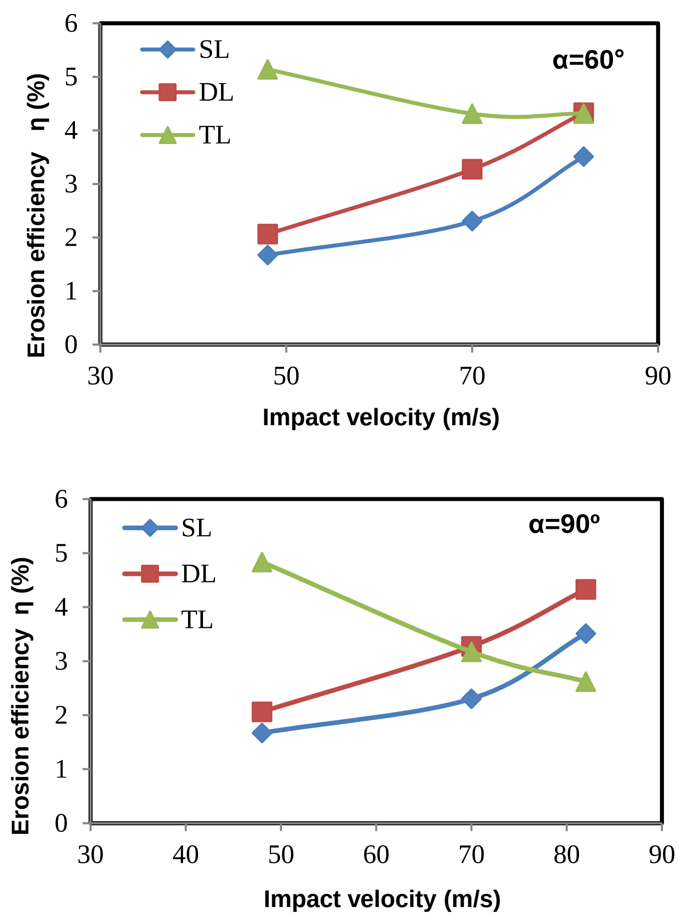

Fig. 5. The erosion efficiency (%) as a function of the impact velocity (m/s) for the LCF-reinforced epoxy composites at impingement angles of (a) 60° and (b) 90°

Surface Morphology of Eroded Surfaces

Figure 6(a) shows the SL composites eroded at a 45° impingement angle with a particle velocity of 82 m/s. It was observed from the SEM imaging that both micro ploughing and micro cutting together were responsible for material removal. Figure 6(b,c) shows the micrographs of the eroded surface of DL and TL composites at a 45° impingement angle with a particle velocity of 82 m/s. It was observed by Sari and Sınmazçelik (2007) that fibres in composites, when subjected to solid particle erosion, encountered intensive debonding and breakage. This was because the fibres in this particular situation were not effectively supported by the matrix material. The same type of behaviour was observed in this experiment; the maximum erosion rate that occurred for the TL composite may have been because of insufficient matrix material.

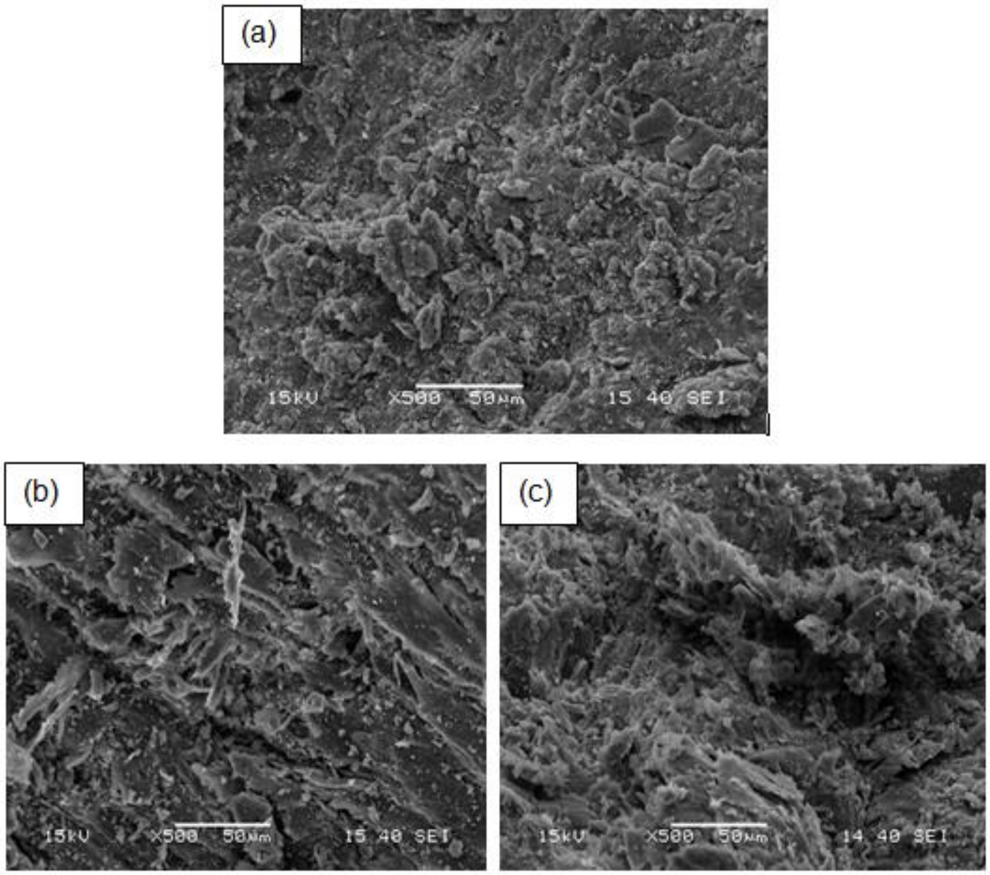

Fig. 6. SEM micrographs of the eroded surface at a 45° impingement angle at an impact velocity of 82 m/s: (a) SL LCF-reinforced epoxy composite; (b) DL LCF-reinforced epoxy composite; and (c) TL LCF-reinforced epoxy composite

CONCLUSIONS

This study investigated solid particle erosion of *Luffa cylindrica* fibre-reinforced epoxy resin composites at various impingement angles and impact velocities, using silica sand as the erodent.

1. The influence of impingement angle on erosive wear of the LCF-epoxy composites under consideration exhibited semi-ductile erosive wear behavior with maximum wear rate at in the range of 45 to 60° impingement angle.
2. The erosion rate for all of the composites increased with increasing impact velocity. It was observed that the erosion rate followed the power law behavior with respect to impact velocity, $E_r = kV^n$, and the value of the velocity exponent n was obtained in the range of 1.2 to 3.3, conforming that the LCF-composite's exhibited a semi-ductile behavior.
3. The erosion efficiency of the LCF- epoxy composites was 1.67% to 4.83% for a 90° impact angle and 2.30% to 5.13% for a 60° impact angle, studied at various impact velocities conforming that the LCF-composite exhibited semi-ductile behavior.

4. The morphology of the eroded surface observed by SEM suggested that the overall erosion damage of the composite is mainly due to breaking of fiber and subsequent removal from the matrix. This removal of fiber might be due to softening of matrix material due to impacting particles velocities. This removal of fiber from the matrix is the result of both micro ploughing and micro cutting due to impacting velocities.

REFERENCES CITED

Arjula, S., and Harsha, A. P. (2006). "Study of erosion efficiency of polymers and polymer composites," *Polym. Test.* 25(2), 188-196. DOI: 10.1016/j.polymertesting.2005.10.009

ASTM D256-10 (2010). "Standard test methods for determining the Izod pendulum impact resistance of plastics," ASTM International, West Conshohocken, PA. DOI: 10.1520/D0256-10.

ASTM D3039/D3039M-14 (2014). "Standard test method for tensile properties of polymer matrix composite materials," ASTM International, West Conshohocken, PA. DOI: 10.1520/D3039_D3039M-14

ASTM D790-03 (2003). "Standard test methods for flexural properties of unreinforced and reinforced plastics and electrical insulating materials," ASTM International, West Conshohocken, PA. DOI: 10.1520/D0790-03

ASTM E384-11e1 (2011). "Standard test method for Knoop and Vickers Hardness of materials," ASTM International, West Conshohocken, PA. DOI: 10.1520/E0384-11E01.

ASTM G76-13 (2013). "Standard test method for conducting erosion tests by solid particle impingement using gas jets," ASTM International, West Conshohocken, PA. DOI: 10.1520/G0076

Bhushan, B. (2013). *Principles and Applications of Tribology,* 2nd Edition, John Wiley & Sons, New York. DOI: 10.1002/9781118403020

Boynard, C. A., Monteiro, S. N., and d'Almeida, J. R. M. (2003). "Aspects of alkali treatment of sponge gourd (*Luffa cylindrica*) fibers on the flexural properties of polyester matrix composites," *J. Appl. Polymer Sci.* 87(12), 1927-1932. DOI: 10.1002/app.11522

Deo, C., and Acharya, S. K. (2009). "Solid particle erosion of *Lantana camara* fiber-reinforced polymer matrix composite," *Polym. Plast. Technol. Engin.* 48(10), 1084-1087. DOI: 10.1080/03602550903094340

El-Shekeil, Y. A., Sapuan, S. M., Abdan, K., and Zainudin, E. S. (2012). "Influence of fiber content on the mechanical and thermal properties of Kenaf fiber reinforced thermoplastic polyurethane composites," *Materials & Design* 40, 299-303. DOI: 10.1016/j.matdes.2012.04.003.

Ghali, L., Msahli, S., Zidi, M., and Sakli, F. (2011). "Effects of fiber weight ratio, structure and fiber modification onto flexural properties of luffa-polyester composites," *Adv. Mater. Phys. Chem.* 1(3), 78. DOI: 10.4236/ampc.2011.13013

Gupta, A., Kumar, A., Patnaik, A., and Biswas, S. (2011). "Effect of different parameters on mechanical and erosion wear behavior of bamboo fiber reinforced epoxy composites," *Int. J. Polym. Sci.* 2011, 592906. DOI: 10.1155/2011/592906

Harsha, A. P., and Thakre, A. A. (2007). "Investigation on solid particle erosion behavior of polyetherimide and its composites," *Wear* 262(7), 807-818. DOI: 10.1016/j.wear.2006.08.012

Karmarkar, A., Chauhan, S. S., Modak, J. M., and Chanda, M. (2007). "Mechanical properties of wood–fiber reinforced polypropylene composites: Effect of a novel compatibilizer with isocyanate functional group," *Comp. Part A: Appl. Sci. and Manufac.* 38(2), 227-233. DOI: 10.1016/j.compositesa.2006.05.005

Li, Q., and Matuana, L. M. (2003). "Surface of cellulosic materials modified with functionalized polyethylene coupling agents," *J. Appl. Polym. Sci.* 88(2), 278-286. DOI: 10.1002/app.11681

Mazali, I. O., and Alves, O. L. (2005). "Morphosynthesis: High fidelity inorganic replica of the fibrous network of loofa sponge (*Luffa cylindrica*)," *Anais da Academia Brasileira de Ciências* 77(1), 25-31.

Mishra, P., and Acharya, S. K. (2010). "Solid particle erosion of bagasse fiber reinforced epoxy composite," *Int. J. Phys. Sci.* 5(2), 109-115.

Mohanta, N., and Acharya, S. K. (2013). "Tensile, flexural and interlaminar shear properties of *Luffa cylindrica* fibre reinforced epoxy composites," *Int. J. Macromol. Sci.* 3, 6-10.

Mohanty, J. R., Das, S. N., Das, H. C., Mahanta, T. K., and Ghadei, S. B. (2014). "Solid particle erosion of date palm leaf fiber reinforced polyvinyl alcohol composites," *Adv. Tribol.* 2014, 293953. DOI: 10.1155/2014/293953.

Oboh, I. O., and Aluyor, E. O. (2009). "*Luffa cylindrica* – An emerging cash crop," *Afri. J. of Agri. Research 4*(8), 684-688.

Ojha, S., Raghavendra, G., and Acharya, S. K. (2014). "A comparative investigation of bio waste filler (wood apple-coconut) reinforced polymer composites," *Polym. Comp.* 35(1), 180-185. DOI: 10.1002/pc.22648

Patel, B. C., Acharya, S. K., and Mishra, D. (2011). "Effect of stacking sequence on the erosive wear behavior of jute and juteglass fabric reinforced epoxy composite," *Int. J. Eng. Sci. Technol.* 3(1), 213-219.

Pool, K. V., Dharan, C. K. H., and Finnie, I. (1986). "Erosive wear of composite materials," *Wear* 107(1), 1-12. DOI: 10.1016/0043-1648(86)90043-8

Partap, S., Kumar, A., Sharma, N. K., and Jha, K. K. (2012). "Luffa cylindrica: An important medicinal plant," *J. of Nat. Prod. & Plant Resources*, 2(1).

Rattan, R., and Bijwe, J. (2007). "Influence of impingement angle on solid particle erosion of carbon fabric reinforced polyetherimide composite," *Wear* 262(5), 568-574. DOI: 10.1016/j.wear.2006.07.001

Rout, J., Misra, M., Tripathy, S. S., Nayak, S. K., and Mohanty, A. K. (2001). "The influence of fibre treatment on the performance of coir-polyester composites," *Compos. Sci. Technol.* 61(9), 1303-1310. DOI: 10.1016/S0266-3538(01)00021-5

Ruff, A. W., and Ives, L. K. (1975). "Measurement of solid particle velocity in erosive wear," *Wear* 35(1), 195-199. DOI: 10.1016/0043-1648(75)90154-4

Samantarai, S., and Acharya, S. K. (2015). *Tribological behavior of rice husk reinforced polymer matrix composite*, Doctoral dissertation, N.I.T. Rourkela.

Satapathy, A., Patnaik, A., and Pradhan, M. K. (2009). "A study on processing, characterization and erosion behavior of fish (*Labeo rohita*) scale filled epoxy matrix composites," *Mater. Des.* 30(7), 2359-2371. DOI: 10.1016/j.matdes.2008.10.033

Sarı, N., and Sınmazçelik, T. (2007). "Erosive wear behavior of carbon fiber /polyetherimide composites under low particle speed," *Mater. Des*. 28(1), 351-355. DOI: 10.1016/j.matdes.2005.05.014

Satyanarayana, K. G., Guimaraes, J. L., and Wypych, F. (2007). "Studies on lignocellulosic fibers of Brazil. Part I: Source, production, morphology, properties and applications," *Compo. Part A: Appl. Sci. and Manufac.* 38(7), 1694-1709. DOI:10.1016/j.compositesa.2007.02.006

Shen, J., Xie, Y. M., Huang, X., Zhou, S., and Ruan, D. (2012). "Mechanical properties of luffa sponge," *J. of the Mech. Behavior of Biomed. Mater.* 15, 141-152. DOI:10.1016/j.jmbbm.2012.07.004.

Shakuntala, O., Raghavendra, G., and Samir, K. A. (2014). "Effect of filler loading on mechanical and tribological properties of wood apple shell reinforced epoxy composite," *Adv. Mater. Sci. Eng.* 2014, 538651. DOI: 10.1155/2014/538651

Srivastava, V. K., and Pawar, A. G. (2006). "Solid particle erosion of glass fibre reinforced flyash filled epoxy resin composites," *Composites Science and Technology* 66(15), 3021-3028. DOI:10.1016/j.compscitech.2006.02.004

Sundararajan, G., Roy, M., and Venkataraman, B. (1990). "Erosion efficiency - A new parameter to characterize the dominant erosion micromechanism," *Wear* 140(2), 369-381. DOI: 10.1016/0043-1648(90)90096-S.

Tewari, U. S., Harsha, A. P., Häger, A. M., and Friedrich, K. (2002). "Solid particle erosion of unidirectional carbon fibre reinforced polyetheretherketone composites," *Wear* 252(11-12), 992-1000. DOI: 10.1016/S0043-1648(02)00063-7

Article submitted: March 20, 2015; Peer review completed: September 22, 2015; Revised version received and accepted: October 12, 2015; Published: October 29, 2015.
DOI: 10.15376/biores.10.4.8364-8377